

Griffiths phases, localization and burstyness in network models

Géza Ódor

MTA-EK-MFA Budapest

16/01/2015 Rio de Janeiro

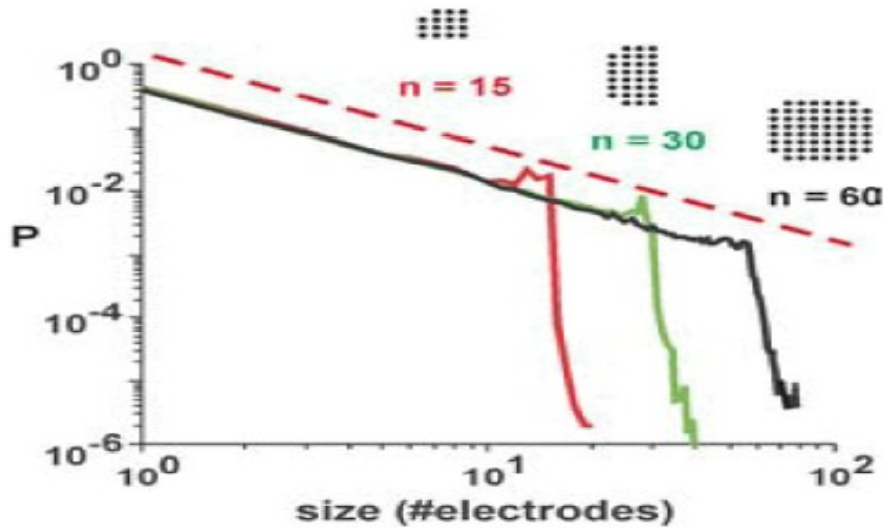
Partners:

<i>R. Juhász</i>	<i>Budapest</i>
<i>M. A. Munoz</i>	<i>Granada</i>
<i>C. Castellano</i>	<i>Roma</i>
<i>R. Pastor-Satorras</i>	<i>Barcelona</i>

Power-laws & critical, slow dynamics observed in networks

- Brain : PL size distribution of neural avalanches

G. Werner : *Biosystems*, 90 (2007) 496,



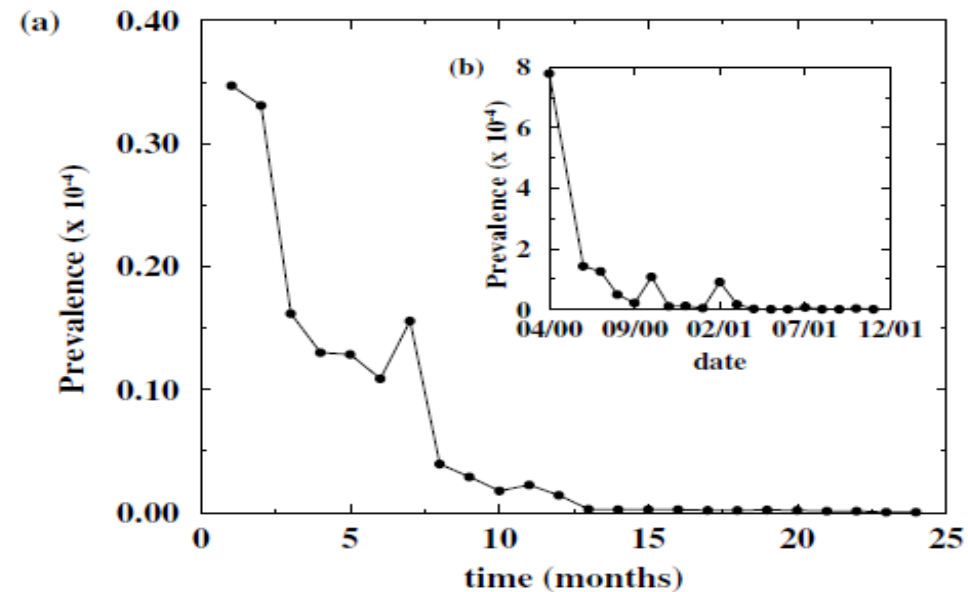
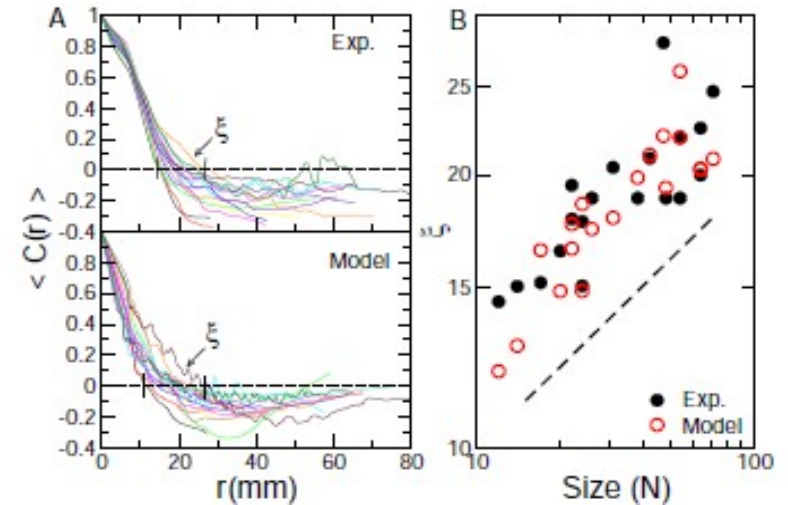
- Internet: worm recovery time is **slow**:

How can we explain power-law dynamics in network models ?

- Correlation length (ξ) diverges

Haimovici et al PRL (2013) :

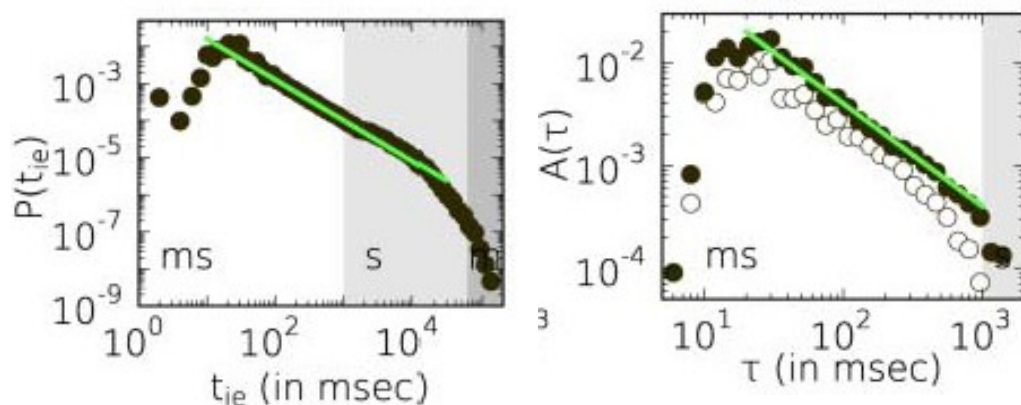
Brain complexity born out of **criticality**.



Burstyness observed in nature

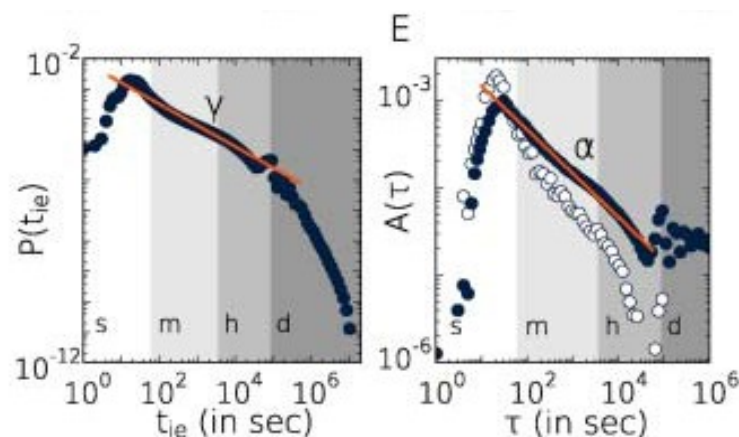
- **Brain** : PL inter-event time distribution of neuron firing sequences & Autocorrelations

Y. Ikegaya et al.: Science, 304 (2004) 559,
N. Takahashi et al.: Neurosci. Res. 58 (2007) 219



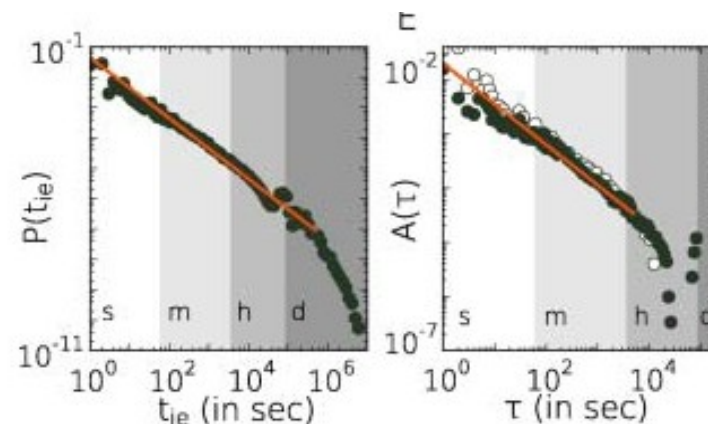
- **Mobile call**: Inter-event times and Autocorrelations

Karsai et al. PRE 83 (2013) 025102 :
Small but slow world ...



- **Internet**: Email sequences:
- And many more
- **Models** exist to explain internal non-Markovian behavior of agents (*Karsai et al.: Sci. Rep. 2 (2012) 397*)

- **Can this occur by the collective behavior of Markovian agents ?**



J. Eckmann et al.: PNAS 101 (2004) 14333

Scaling in nonequilibrium system

Scaling and universality classes appear in complex system due to : $\xi \rightarrow \infty$
i.e: near critical points, due to currents, ...

Basic models are classified by **universal scaling behavior** in Euclidean, regular system

- **Why don't we find these critical universality classes in dynamical network models ?**
- **Power laws are frequent in nature**
↔ Tuning to critical point (SOC) ?

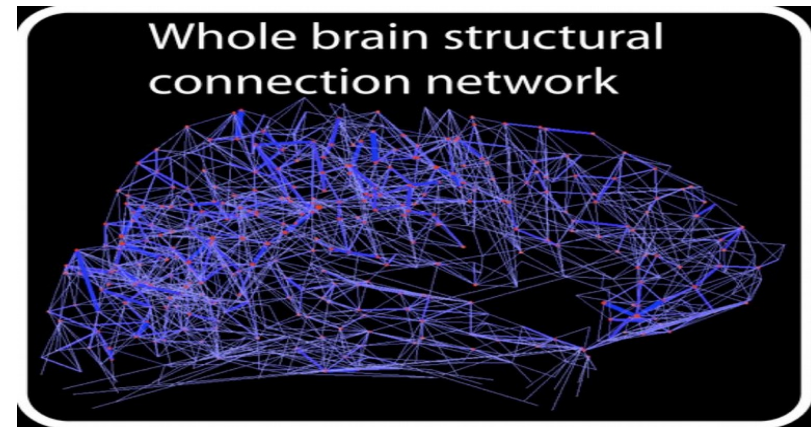
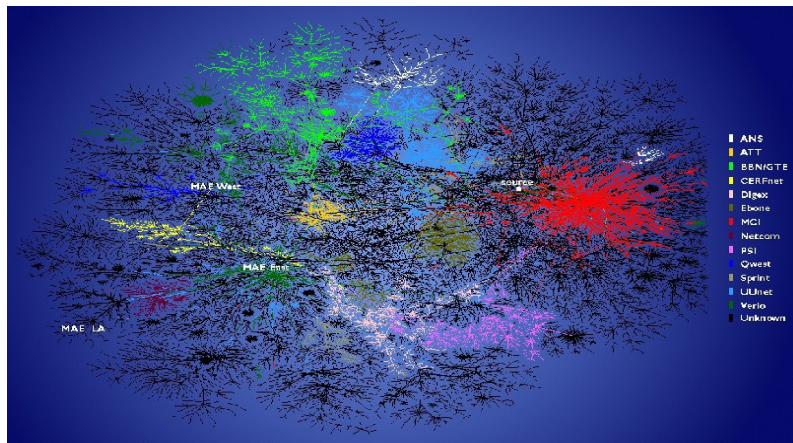
I'll show a possible way to understand these in case of quasi-static networks



Dynamical models on networks

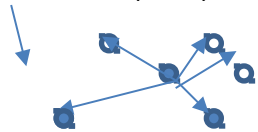
Small world networks:

Expectation: mean-field type behavior with fast dynamics

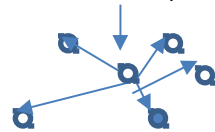


Prototype: **Susceptible-Infected-Susceptible (SIS)** two-state model:

Infect: $\lambda / (1+\lambda)$



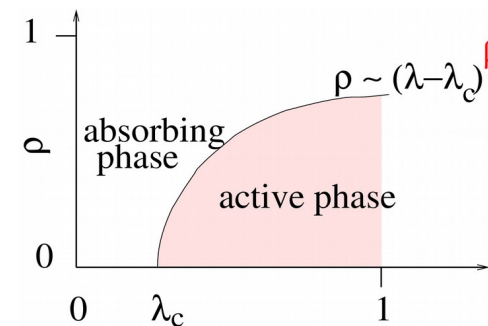
Heal: $1 / (1+\lambda)$



Order parameter : density of active (●) sites

Regular, Euclidean lattice: **DP** critical point : $\lambda_c > 0$ between inactive and active phases

For SIS : Infections attempted for all nn



Rare region effects in networks ?

Rare active regions below λ_c with: $\tau(\mathbf{A}) \sim e^A$
→ slow dynamics (Griffiths Phase) ?

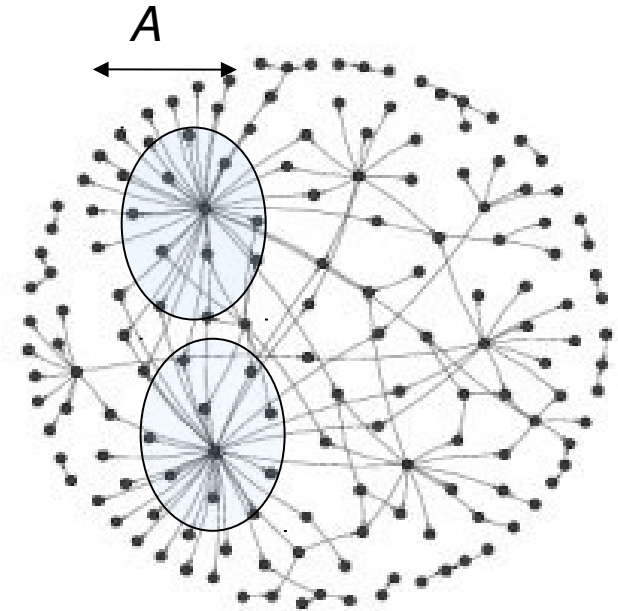
$$\rho(t) \sim \int d\mathbf{A}_R A_R p(\mathbf{A}_R) \exp[-t/\tau]$$

M. A. Munoz, R. Juhász, C. Castellano and G. Ódor, PRL 105, 128701

1. Inherent disorder in couplings
2. Disorder induced by topology

Optimal fluctuation theory + simulations: **YES**

- In weighted Erdős-Rényi random networks
- In networks with **finite topological dimension**



Quenched Mean-Field (QMF) theory for SIS

Rate equation of SIS for occupancy prob. at site i :

$$\frac{d\rho_i(t)}{dt} = -\rho_i(t) + \lambda(1 - \rho_i(t)) \sum_{j=1}^N A_{ij} w_{ij} \rho_j(t)$$

Weighted (real symmetric) Adjacency matrix:

$$B_{ij} = A_{ij} w_{ij},$$

For $t \rightarrow \infty$ the system evolves into a steady state, with the probabilities expressed as

$$\rho_i = \frac{\lambda \sum_j B_{ij} \rho_j}{1 + \lambda \sum_j B_{ij} \rho_j}. \quad (5)$$

Express ρ_i on orthonormal eigenvector ($\mathbf{f}_i(\Lambda)$) basis:

$$\rho_i = \sum_{\Lambda} c(\Lambda) f_i(\Lambda). \quad (6)$$

Mean-field critical point estimate

$$\lambda_c = 1/\Lambda_1$$

Total infection density vanishes near λ_c as :

$$\rho(\lambda) \approx \alpha_1 \tau + \alpha_2 \tau^2 + \dots, \quad (8)$$

where $\tau = \lambda \Lambda_1 - 1 \ll 1$ with the coefficients

$$\alpha_j = \sum_{i=1}^N f_i(\Lambda_j) / [N \sum_{i=1}^N f_i^2(\Lambda_j)]. \quad (9)$$

To describe the localization of the components of $\mathbf{f}(\Lambda_1)$ [19] used the inverse participation ratio

$$IPR(\Lambda) \equiv \sum_{i=1}^N f_i^4(\Lambda), \quad (10)$$

QMF results for SIS on Erdős-Rényi graphs

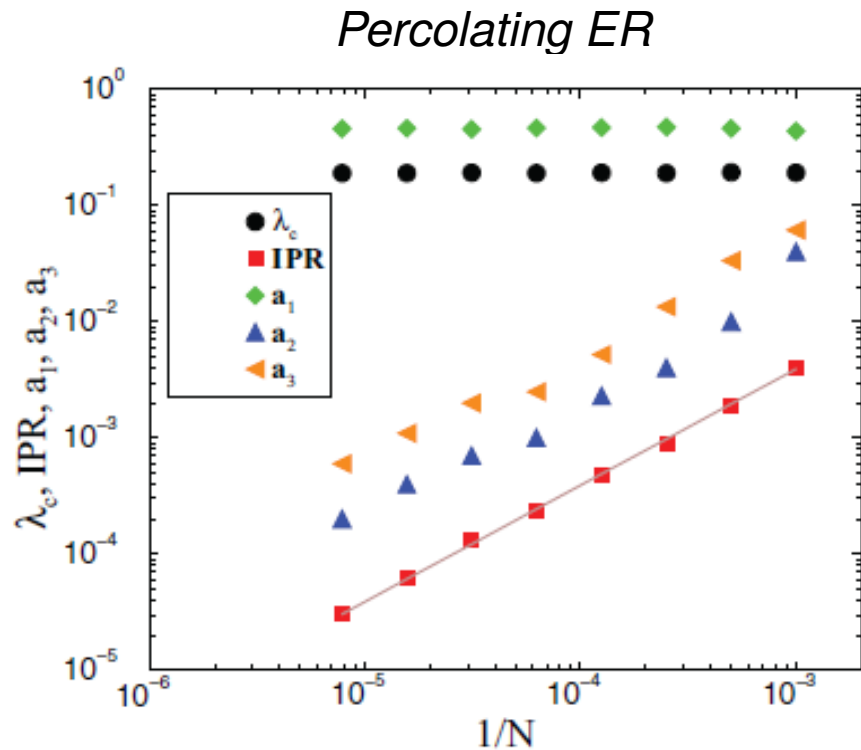


FIG. 1. (Color online) Finite size scaling of QMF results on the ER model with $\langle k \rangle = 4$ for $N = 1000, 2000, 4000, \dots, 128\,000$. Bullets, λ_c ; boxes, IPR; up-triangles, a_1 ; down-triangles, a_2 ; right-triangles, a_3 . (Line) Least-squares fitting with the form $\sim 1/N$.

$IPR \sim 1/N \rightarrow$ delocalization

$$\Lambda_1 = 1/\lambda_c \rightarrow 5.2(2) \leftrightarrow \Lambda_1 = \langle k \rangle = 4$$

$$a_1 \gg a_2, a_3, \dots$$

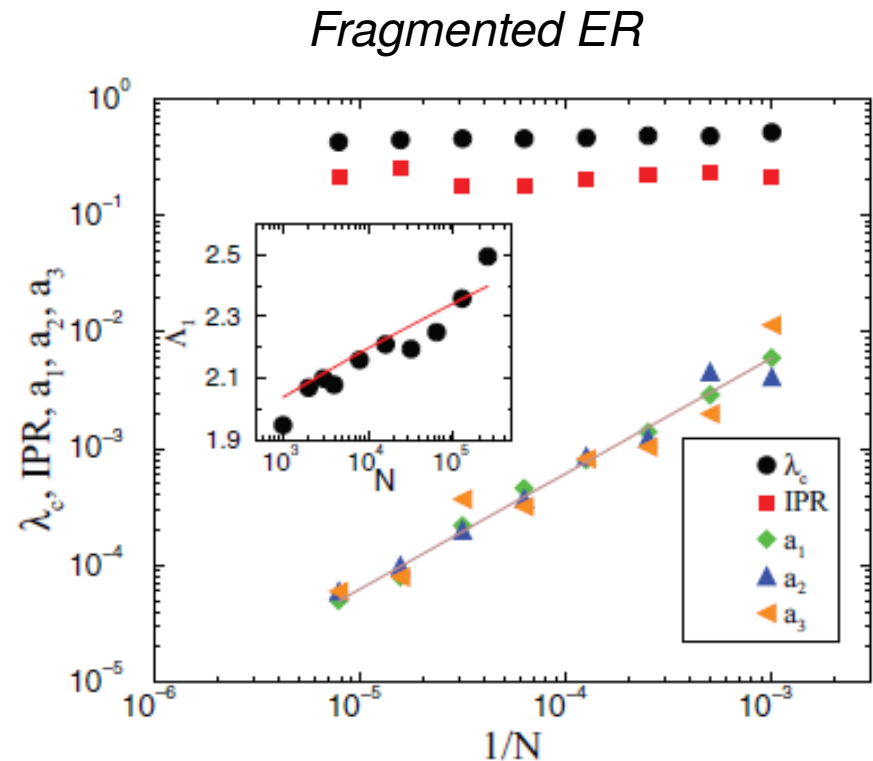


FIG. 3. (Color online) Finite size scaling of QMF results for ER graph with $\langle k \rangle = 0.3N = 1000, 2000, 4000, \dots, 128\,000$. Bullets, λ_c ; boxes, IPR; up-triangles, a_1 ; down-triangles, a_2 ; right-triangles, a_3 . (Line) Least-squares fitting with a form $1/N$. (Inset) $\Lambda_1(N)$ (bullets) and the form (8) (line).

$IPR \rightarrow 0.22(2) \rightarrow$ localization

$$\Lambda_1(N) = \sqrt{\ln N / \ln \ln N}$$

$a_1 \sim a_2 \sim a_3$: strong corrections to scaling,

Density decay simulation results on ER graphs

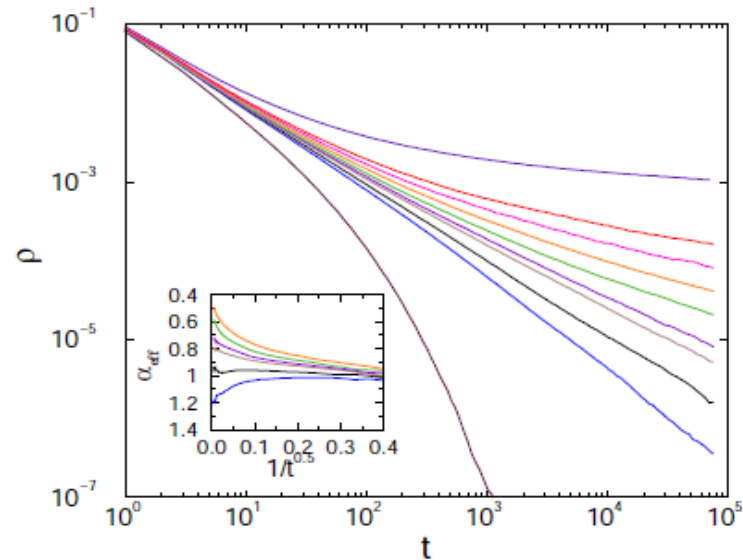


FIG. 2: (Color online) Density decay as a function of time for the SIS on ER graph with $\langle k \rangle = 1$. Network size $N = 10^6$. Different curves correspond to $\lambda = 1.05, 1.09, 1.095, 1.1, 1.02, 1.05, 1.095, 1.115, 1.12, 1.15$ (from bottom to top curves). Inset: effective exponents of the same data near the phase transition point.

Percolating ER

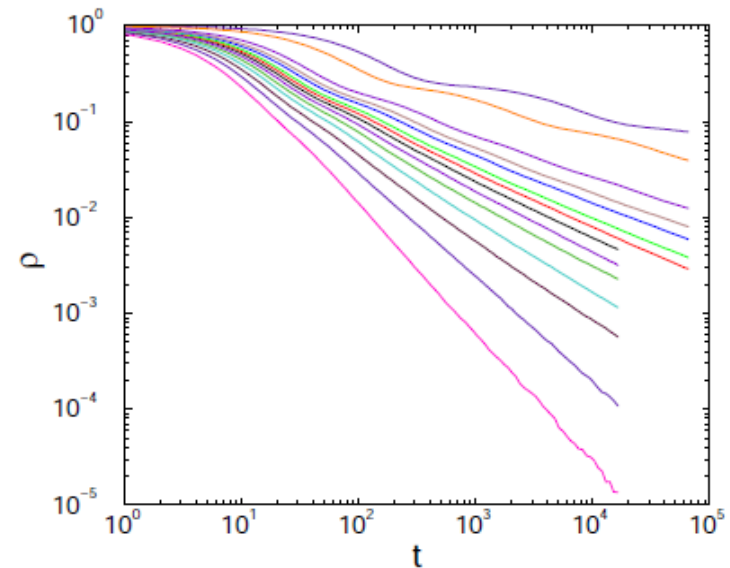


FIG. 4: (Color online) Density decay as a function of time in the SIS defined on ER graph with $\langle k \rangle = 0.3$. Network size $N = 10^6$. Different curves correspond to $\lambda = 4, 5, 6, 7, 8, 9, 10, 11, 12, 14, 16, 20, 50, 100$ (from bottom to top curves).

Fragmented ER

Quenched Mean-Field for SIS on scale-free BA graph

Barabási-Albert graph lin. attachment prob.:

$$P_{s \rightarrow s'} = k_{s'} / \sum_{s'' < s} k_{s''}$$

$$P(k) \sim k^{-3} \quad \Lambda_1(N) \sim N^{1/4}$$

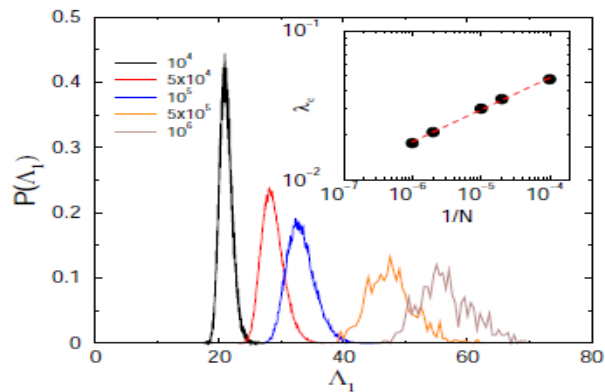


FIG. 6: (Color online) Probability distribution of IPR of the $m = 3$ BA SIS model for sizes $N = 10^4$, 5×10^4 , 10^5 , 5×10^5 and $N = 10^6$ (from left to right).

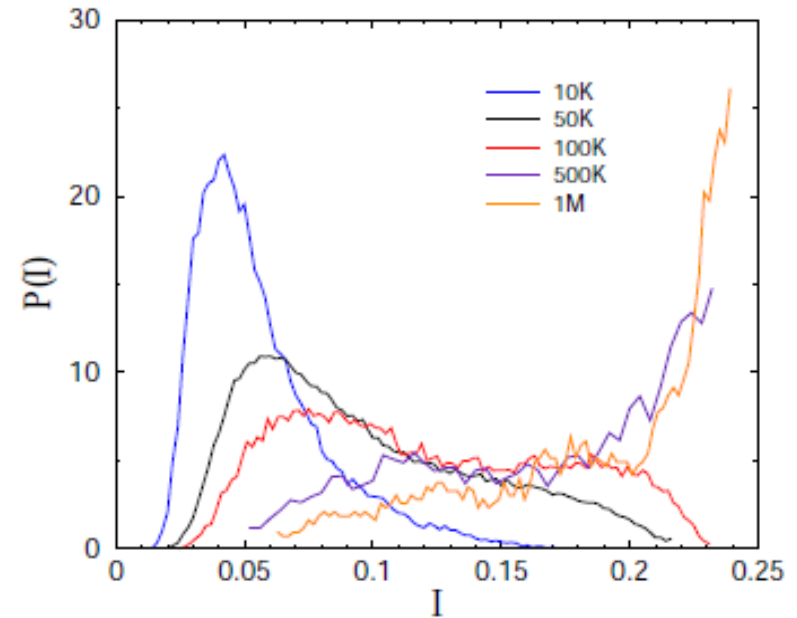


FIG. 6: (Color online) Probability distribution of IPR of the $m = 3$ BA SIS model for sizes $N = 10^4$, 5×10^4 , 10^5 , 5×10^5 and $N = 10^6$ (from left to right).

IPR exhibit wide distributions
Localization for $N \rightarrow \infty$

Rare-region effects in aging BA graphs

BA followed by preferential edge removal

$$p_{ij} \propto k_i k_j$$

dilution is repeated until 20% of links are removed

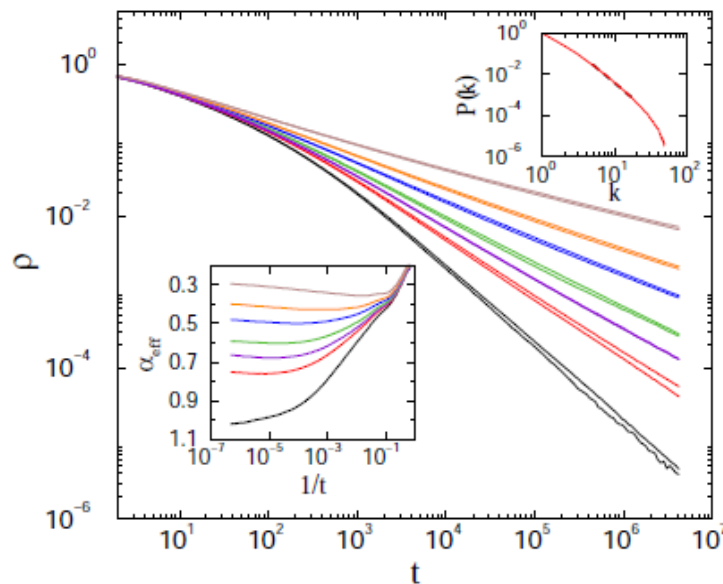


FIG. 7: (Color online) Density decay as a function of time for the SIS on BA graph with network sizes: $N = 10^5$ (thin lines), $N = 10^6$ (thick lines). Different curves correspond to $\lambda = 2.4, 2.45, 2.47, 2.5, 2.55, 2.6, 2.7$ (from bottom to top curves). Left inset: Local slopes of the same data. Right inset: Degree distribution of the aging BA graph for $N = 4 \times 10^6$ nodes.

No size dependence \rightarrow Griffiths Phase

QMF

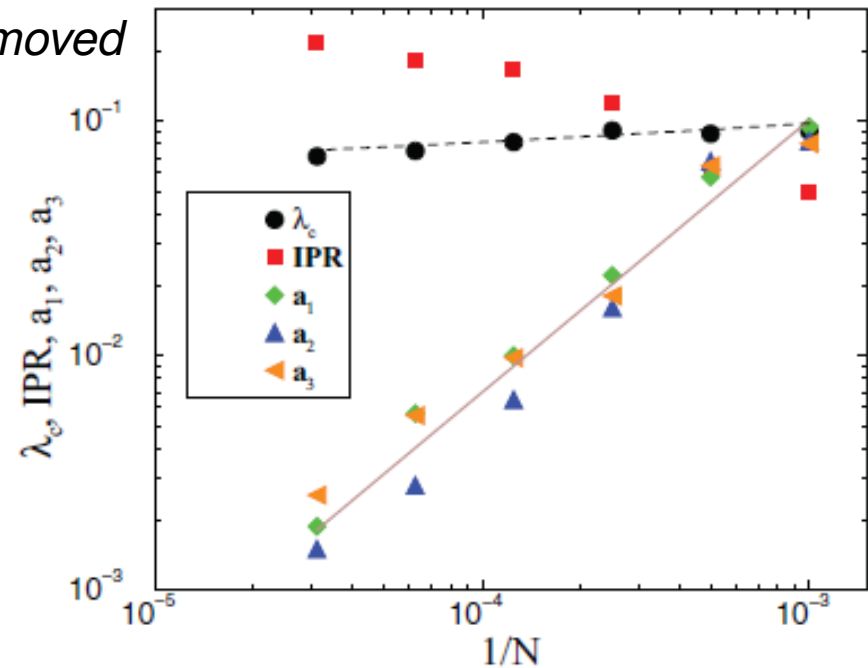


FIG. 6. (Color online) Finite size scaling of QMF SD results of the SIS on generalized BAT with $N = 1000, 2000, 4000, 8000, 16000, 32000$ nodes. Bullets, λ_c ; boxes, IPR; up-triangles, a_1 ; down-triangles, a_2 ; right-triangles, a_3 . (Line) Least-squares fitting with the form $\sim 1/N$.

$$\lambda_c = 1/\Lambda_1 = 0.001 + 0.17(1/N)^{0.18}$$

IPR $\rightarrow 0.28(5)$

Localization in the steady state

Bursts in the SIS model in one-dimension

- Density decay and seed simulations of SIS on a ring at the critical point
- Power-law inter-event time (Δ) distribution among subsequent infection attempts
- Invariance on the time window and initial conditions
- The tail distribution decays as the known auto-correlation function for $t \rightarrow \infty$

$$P(\Delta) \simeq p^2 \Gamma(t, s)$$

$$\Gamma(t, s) = \langle n_i(t)n_i(s) \rangle - \langle n_i(t) \rangle \langle n_i(s) \rangle$$

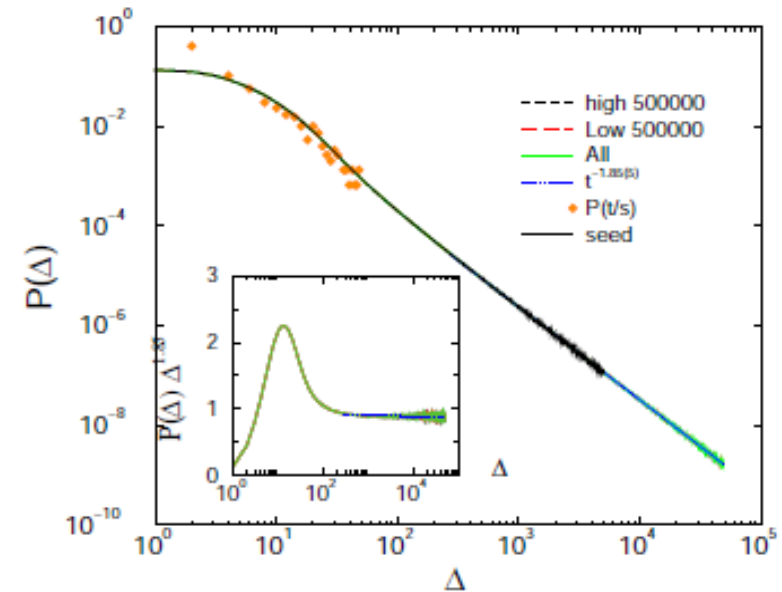


FIG. 1: (Color online) Inter-communication time distribution in the 1d critical CP of size $N = 10^5$. Full line denote histogramming from all times, dashed line from high times, long dashes from low times. The dotted line shows a power-law fit for $t > 200$ resulting in $\propto t^{-1.85(5)}$. The solid thin line corresponds to runs from seed initial conditions. Inset: the same data multiplied by the $t^{1.85}$ corresponding to the tail decay.

$$\Gamma(t, s) \propto (t/s)^{-\theta} = (\Delta/s + 1)^{-\theta}$$

Bursts of the SIS in Generalized Small World networks



$$P(l) \sim \beta l^{-2}$$

- Density decay and seed simulations of SIS on a near the critical point
- Power-law inter-event time (Δ) distribution among subsequent infection attempts
- Invariance on the time window and initial conditions
- The tail distribution decays with a λ dependent exponent around the critical point **in the extended Griffiths Phase**

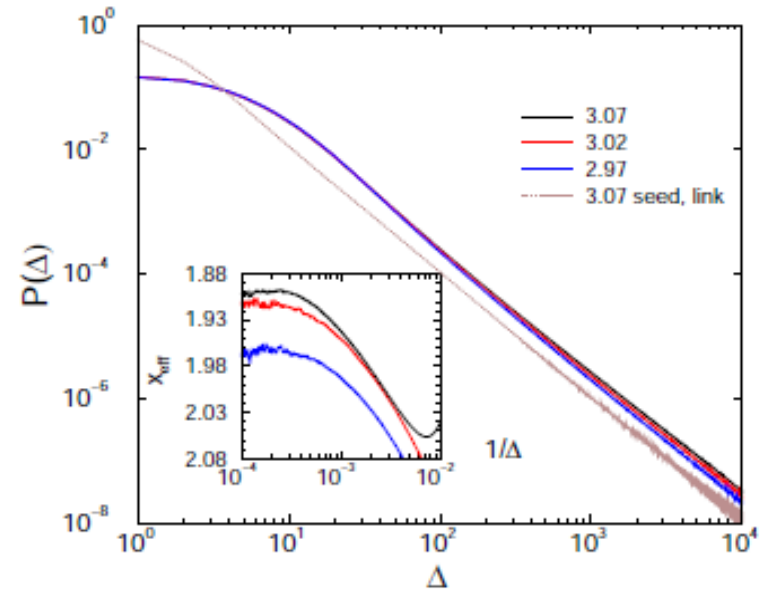


FIG. 2: (Color online) Inter-communication time distribution in the GP of a GSW network with $\beta = 0.1$ of size $N = 10^6$ and $\lambda = 2.97, 3.02, 3.07$ (bottom to top solid curves). The solid thin line corresponds to runs from seed initial conditions measuring all activation attempts. Inset: Effective exponents defined as (4) of the same data.

Bursts of the SIS in aging scale-free networks

- Barabasi-Albert model with preferential detachment of aging links: $P(k) \sim k^{-3} \exp(-ak)$
- Density decay simulations of SIS on a near the critical point
- Power-law inter-event time (Δ) distribution among subsequent infection attempts
- The tail distribution decays with a λ dependent exponent around the critical point **in an extended Griffiths Phase**

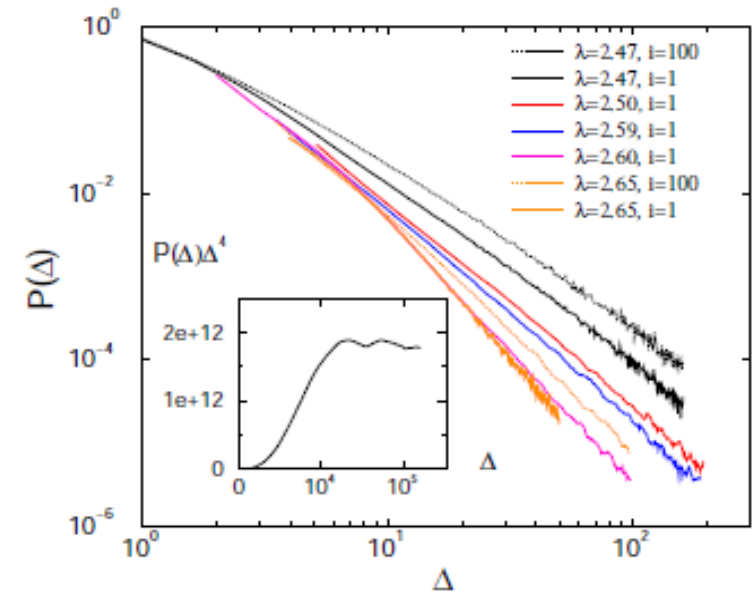


FIG. 4: (Color online) Inter-communication time distribution in the GP of an ageing BA network of size $N = 10^5$ for $\lambda = 2.47, 2.5, 2.55, 2.59, 2.6, 2.65$ (top to bottom curves) and measured at different ($i = 1$ and $i = 100$) sites. Power-law fitting exponents for the tail behavior is shown in the text. Inset: $P(\Delta)\Delta^4$ at the λ_c of the CP defined on the pure BA graph.

Summary

- **Quasi-static disorder** in complex networks can cause slow (PL) **dynamics** :
Rare-regions, Griffiths phases in extended regions → **without SOC mechanism !**
- **GP** can occur due to **purely topological disorder in finite dimensional network models**
- In **infinite dimensional** networks (ER, BA) **mean-field transition** of SIS with logarithmic corrections (HMF, simulations, QMF), **but localization for $\gamma > 3$**
- In **weighted BA trees** non-universal, slow, power-law dynamics can occur for finite N , but in the $N \rightarrow \infty$ limit: saturation occurs
- **GP** is related to **localization** in the steady state in most cases
- **Bursty behavior in extended GP-s** as a consequence of heterogeneity + $\tau \rightarrow \infty$
Complexity induces non-Markovian behavior of the agents of the network

[1] M. A. Munoz, R. Juhász, C. Castellano, G. Ódor, *Phys. Rev. Lett.* 105 (2010) 128701

[2] R. Juhász, G. Ódor, C. Castellano, M. A. Munoz, *Phys. Rev. E* 85 (2012) 066125

[3] G. Ódor, R. Pastor-Satorras, *Phys. Rev. E* 86 (2012) 026117

[4] G. Ódor, *Phys. Rev. E* 87, 042132 (2013)

[5] G. Ódor, *Phys. Rev. E* 88, 032109 (2013)

[6] G. Ódor, *Phys. Rev. E* 89, 042102 (2014)

[7] G. Ódor, *Phys. Rev. E* 90, 032110 (2014)



SIS on weighed Barabási-Albert graphs

- Excluding loops slows down the spreading
- WBAT-II: disassortative weight scheme

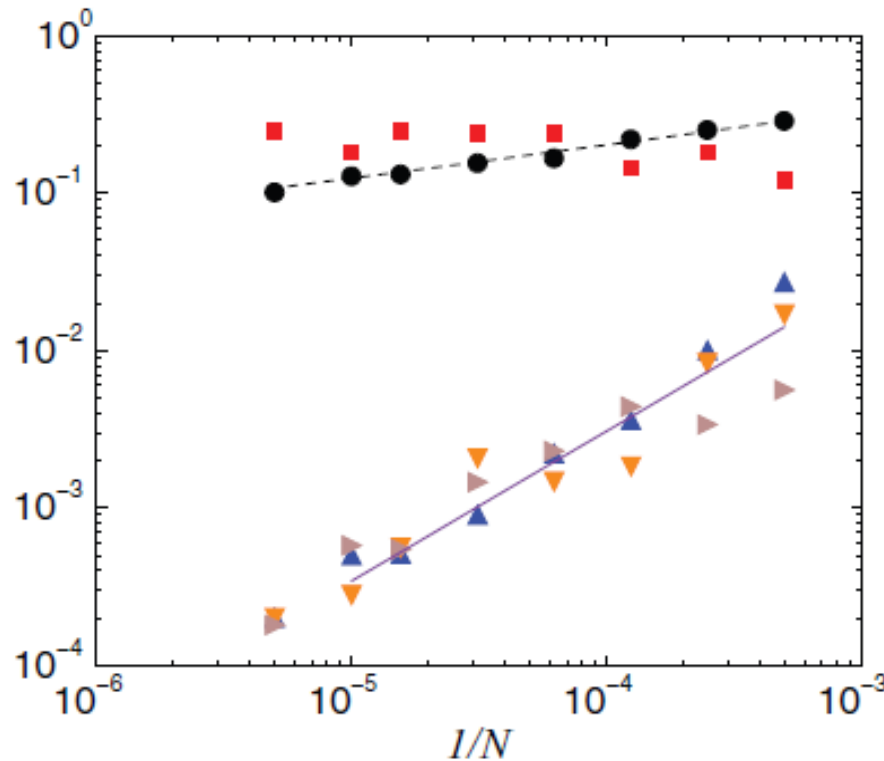


FIG. 2. (Color online) Finite-size scaling of QMF SD results for WBAT-II model for $N = 2\,000, 4\,000, \dots, 200\,000$. Bullets, λ_c ; boxes, IPR; up-triangles, a_1 ; down-triangles, a_2 ; right-triangles, a_3 . Lines: least-squares fitting for with the form Eq. (12).

Weights: $\omega_{ij} = \frac{|i-j|^x}{N}$, $k_i \propto (N/i)^{1/2}$

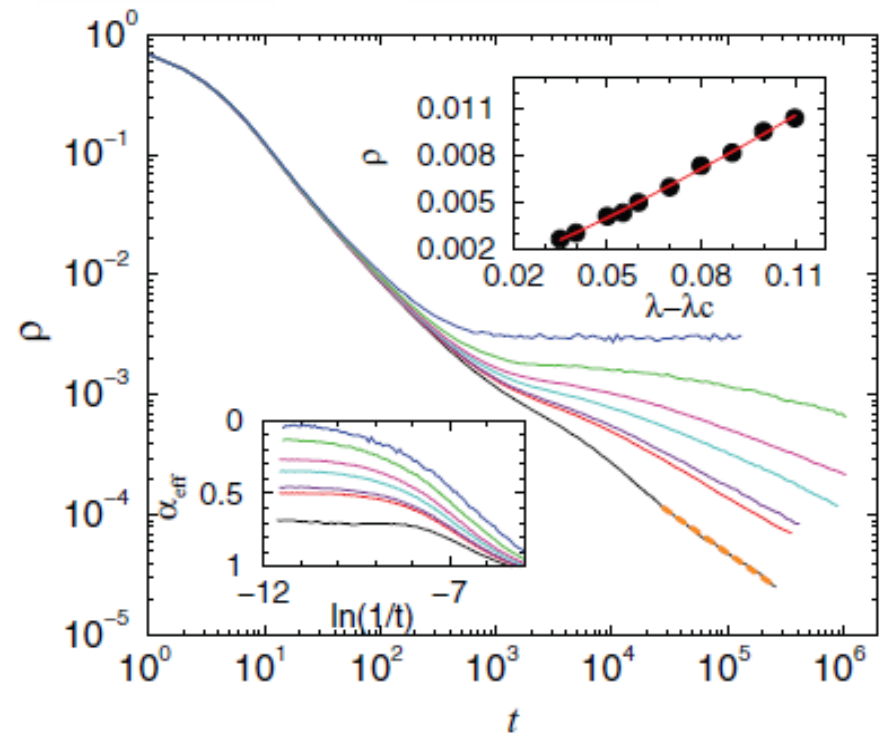


FIG. 4. (Color online) Density decay as a function of time for the SIS on weighted BA trees generated with the age-dependent (disassortative) WBAT-II scheme with exponent $x = 2$. Network size $N = 10^6$. Different curves correspond to $\lambda = 1.657, 1.66, 1.661, 1.663, 1.67, 1.68, 1.69$ (from bottom to top). Dashed line: power-law fit. Left inset: Local slopes of the same curves showing level-off for large times. Right inset: Steady-state density (bullets) above the epidemic threshold. The line shows power-law fitting with the form Eq. (14).

*λ dependent density decay exponents:
Griffiths Phases or Smeared phase transition ?*

Rare Region theory for **quench disordered CP**

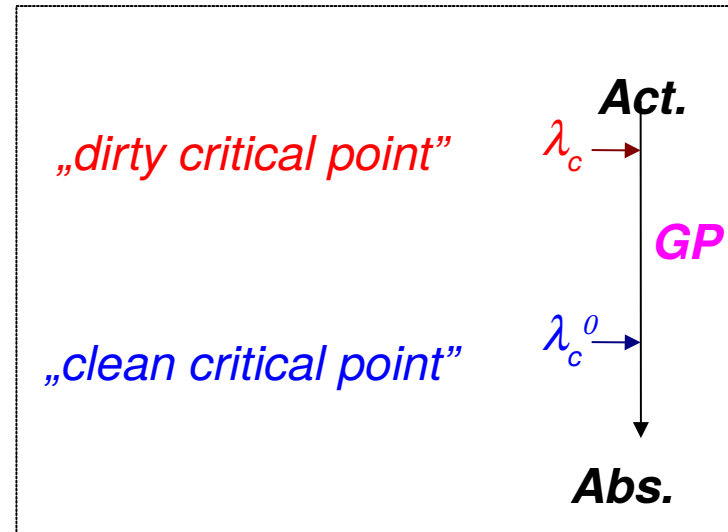
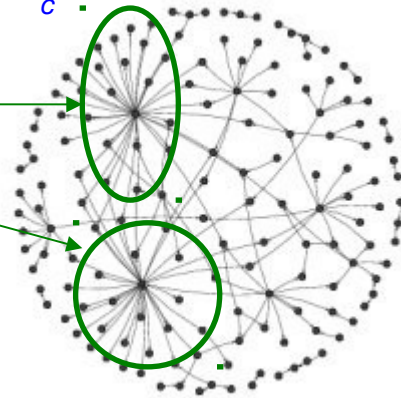
- Fixed (quenched) disorder/impurity changes the local birth rate $\Rightarrow \lambda_c > \lambda_c^0$.

- **Locally active**, but arbitrarily large Rare Regions

in the inactive phase due to the **inhomogeneities**

- Probability of RR of size L_R :

$$w(L_R) \sim \exp(-c L_R)$$



contribute to the density: $\rho(t) \sim \int dL_R L_R w(L_R) \exp[-t/\tau(L_R)]$

- For $\lambda < \lambda_c^0$: conventional (exponentially fast) decay

- At λ_c^0 the characteristic time scales as: $\tau(L_R) \sim L_R^Z \Rightarrow$ saddle point analysis:

$$\ln \rho(t) \sim t^{d/(d+Z)}$$

stretched exponential

- For $\lambda_c^0 < \lambda < \lambda_c$:

$$\tau(L_R) \sim \exp(b L_R):$$

Griffiths Phase

$$\rho(t) \sim t^{-c/b}$$

continuously changing exponents

- At λ_c : b may diverge $\rightarrow \rho(t) \sim \ln(t)^{-\alpha}$ Infinite randomness fixed point scaling

- In case of correlated RR-s with dimension $> d$: smeared transition